AUT Journal of Electrical Engineering

AUT J. Electr. Eng., 55(2) (2023) 241-254
DOI: 10.22060/eej.2023.22360.5536

Application of ANFIS Technique for Wide-Band Modeling of Overvoltage of Single-Conductor Overhead Lines with Arrester above Dispersive and Two-Layer Soils

Saeed Reza Ostadzadeh*

Faculty of Engineering, Arak University, Arak, Iran.

ABSTRACT: In this paper, an efficient closed-form expression for overvoltage of overhead lines under direct strike in the presence of lightning arresters is presented. The lightning arresters are also grounded via two grounding systems namely vertical electrode and horizontal grid. The simulation results based on the exact method show that among different parameters, the resistivity of soil and line height affect the overvoltage. To extract the closed-form expression, adaptive-network-based fuzzy inference systems (ANFIS) are used. In creating the ANFIS-based expression, it is first assumed that the electrical parameters of the soil are constant. Then a number of input-output pairs (inputs are soil resistivity and line height and the output is overvoltage) are computed from exact methods to train the algorithm. Once the algorithm is converged, the efficient expression is extracted. This simple expression can be easily used in dispersive soils (frequency-variant electrical parameters) and horizontally two-layered soils (non-homogenous electrical parameters) provided that the equivalent frequency and equivalent resistivity concepts respectively in dispersive and two-layer soils are used.

Review History:

Received: Apr. 27, 2023
Revised: Aug. 18, 2023
Accepted: Aug. 19, 2023
Available Online: Oct. 01, 2023

Keywords:

Overhead line
Arrester
Dispersive
Two-layer
Overvoltage
ANFIS

1- Introduction

Overvoltage of overhead lines subject to lightning strokes is a leading cause of short circuits and line outages in transmission systems [1]. Its computation is of importance due to its application in the insulation coordination study of power systems and the selection of respective lightning arresters. However, it is generally a difficult task because of the impulse characteristics of grounding systems and the nonlinear behavior of the arresters.

There are several approaches either in the frequency domain [2-4] or in the time domain [5-7]. The frequency-domain methods can easily incorporate the frequency dependence of electrical parameters of soil (dispersive soil) [3]. The time domain methods, on the other hand, are capable of treating nonlinear elements [6, 7]. However, they are inappropriate in including the dispersion of lossy soils. All mentioned methods suffer from time-consuming computations especially when the weather conditions are changed. To this end, a hybrid approach based on combining the Baum–Liu–Tesche (BLT) equations and the arithmetic operator method (AOM) has been proposed [8]. Since the BLT equations are based on the transmission line (TL) approximation, it is thus restricted to conditions at which kh<<1 (k is wave number and h is the transmission line-height) [9], elsewhere it yields to violated results. It means that it is acceptable for slow-fronted currents containing lower frequency content with respect to fast-fronted currents, or low-valued heights. Also, AOM is an iterative method [10], the authors in [11] proposed an efficient hybrid model based on combining the method of fuzzy (MoF) and intelligent water drop algorithm (IWD) to overcome the mentioned drawbacks.

To the best of my knowledge, there is no formula for the overvoltage of overhead lines with arrester termination except the one in [12, 13] extracted without considering the arrester based on curve-fit methods. Hence, without losing generality, a qualitative model based on adaptive-network-based fuzzy inference systems (ANFIS) [14] for predicting the overvoltage only for direct strike is proposed. The same approach can be similarly carried out for indirect strikes. Using this model, the overvoltage across the arrester in the presence of soil of constant electrical parameters is first efficiently computed. After that, using the approximation of equivalent frequency in dispersive soils [15], and the equivalent resistivity concept in two-layer soils [16], the effects of dispersion and in-homogeneity separately and simultaneously can be easily integrated with the first-created model.

This paper is organized as follows. In section 2, exact and approximate models for the problem under consideration are proposed. Section 3 is focused on the sensitivity analyses of the parameters affecting the overvoltage. Section 4 investigates the accuracy of simulation results based on the ANFIS model. As the last final achievement of this study, the capability of the proposed model in dispersive and in-homogenous soils is investigated in section 5. Finally, conclusions are given in section 6.

*Corresponding author's email: s-ostadzadeh@araku.ac.ir

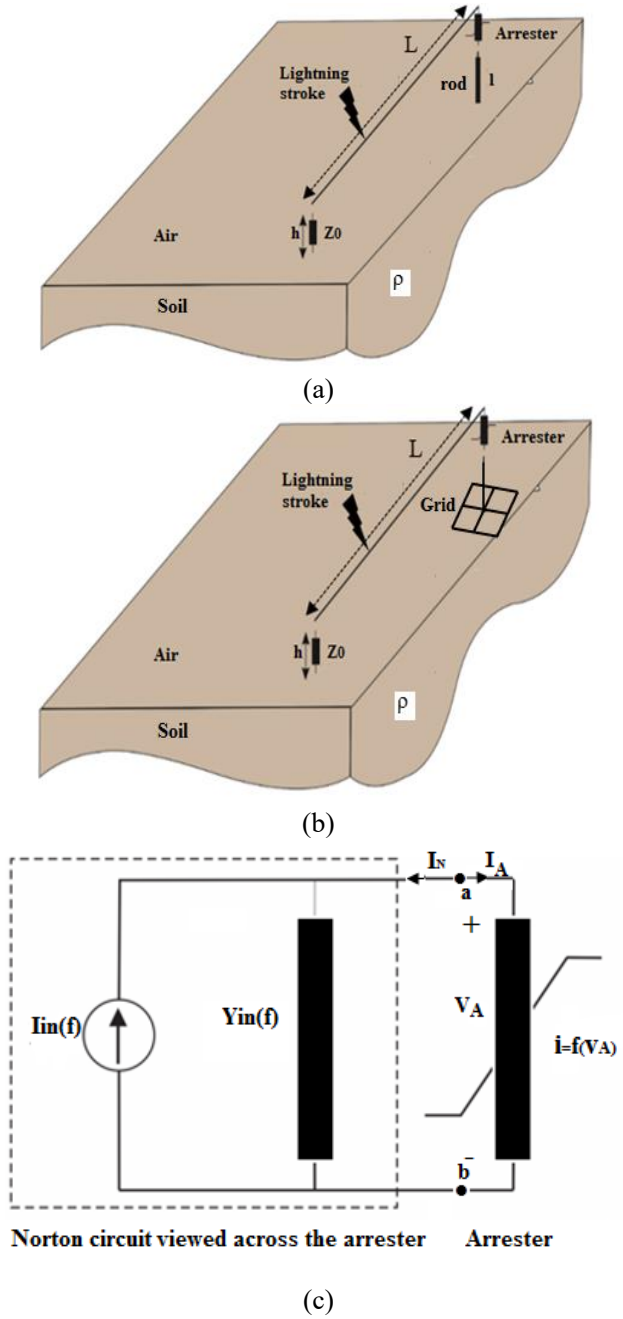

Fig. 1. A transmission line under direct strike with an arrester grounded with (a): a vertical rod, and (b): a grid as well as (c); a nonlinear microwave circuit for Figs. 1(a) and (b), [8].

2- MODELING PRINCIPLES

Fig. 1 shows the schematic of the single-conductor overhead line terminated to an arrester as well as its microwave equivalent circuit. In Fig. 1(a) and (b), the overhead line with length L is located at height h from a lossy soil with resistivity ρ and relative permittivity ε_r. It is also matched at the left side via a characteristic impedance Z_0, while at the right side, it is ended with an arrester. The arrester is connected to a vertical rod of length l and a 2×2 grid as shown respectively in Figs. 1(a) and (b). The microwave equivalent circuit in Fig. 1(c) consists of two parts. The first part is a Norton equivalent circuit viewed across the arrester, while the second part is a nonlinear load to model the arrester.

Note that the wide-band input impedance of the two grounding systems is included in Fig.1(c) below

$$I_{sc} = \frac{I_{sc}^{TL}}{1 + Z_{in}^{G} Y_{in}^{TL}} \tag{1}$$

$$Y_{in} = \frac{Y_{in}^{TL}}{1 + Z_{in}^{G} Y_{in}^{TL}} \tag{2}$$

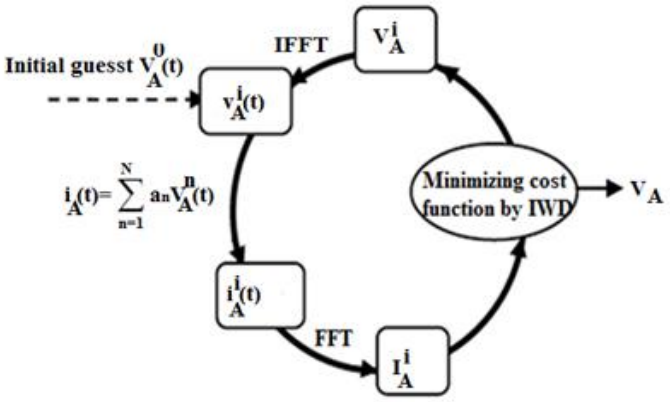

Fig. 2. Iteration process in the exact model for computing overvoltage.

In (1), and (2), I_{sc}^{T} , and Y_{in}^{T} are respectively short circuit current and input admittance of the transmission line, while Z_{in}^{G} is the input impedance of the two grounding systems.

In this section, exact and approximate models respectively based on [11] and ANFIS for computing the overvoltage is briefly presented.

2- 1- Exact Model

In the exact model, at first, applying KCL in the frequency domain at node 'a' in Fig. 1 (c) yields:

$$I_N + I_A = 0 \tag{3}$$

Where I_N and I_A are respectively Norton's circuit and arrester current vectors. Substituting I_N from Fig. 1(c) in (1), we have

$$-\bar{I}_{in} + \bar{\bar{Y}}_{in} \times \bar{V}_{NL} + \bar{I}_A = 0 \tag{4}$$

Where $\bar{\bar{Y}}_{in}$ is the input admittance matrix at mixing frequencies. Also, $\bar{I}_{in}$ is computed only at k exciting frequencies inside the lightning current content, i.e.

$$\bar{I}_{in} = [I_{in,0} \;\; , I_{in,1}, ...I_{in,k} ... 0 \;\; 0] \tag{5}$$

whereas $\bar{I}_A$ and $\bar{V}_A$ are computed at k′ mixing frequencies (k′>k), i.e.,

$$(5)\; \bar{I}_{in} = [I_{in,0} \;\; , I_{in,1}, ...I_{in,k} ... 0 \;\; 0] \tag{6}$$

$$\bar{V}_A = [V_{A,0} \;\; , V_{A,1}, ...V_{A,2k'}]; \tag{7}$$

The corresponding time-domain expressions for the above mentioned quantities are as below

$$i_A(t) = I_{A,0} + (\sum_{n=1}^{k'} I_{A,2p-1} \cos\omega_p t + I_{A,2p} \sin\omega_p t) \tag{8}$$

$$v_A(t) = v_{A,0} + (\sum_{p=1}^{k'} v_{A,2p-1} \cos\omega_p t + v_{A,2p} \sin\omega_p t) \tag{9}$$

In (4), $\bar{I}_A$ can be expressed versus V_A in the frequency domain as below

$$\varepsilon = -\bar{I}_{in} + \bar{\bar{Y}}_{in} \times \bar{V}_{NL} + \bar{T}f(\bar{T}^{-1} V_A) \to 0 \tag{10}$$

Where $\bar{T}$ and $\bar{T}^{-1}$ are transformation matrices from time domain to frequency domain and vice versa. Substituting (9) in (4), the following cost function is achieved.

$$\mu(x) = \exp\left[-\left(\frac{x - c_i}{\sigma_i}\right)^2\right] \tag{11}$$

Solving the above cost function based on IWD algorithm [17-19], $\bar{V}_A$ and accordingly $v_A(t)$ is computed. Fig. 2 shows the flow chart of the exact model.

2- 2- Approximate Model

In contrast with the exact model, an efficient approximate model based on the ANFIS algorithm could be used. ANFIS is a class of adaptive networks that are functionally equivalent to fuzzy inference systems (FIS). The ANFIS architecture consists of a fuzzy layer, product layer, normalized layer, defuzzy layer, and summation layer. A typical architecture of ANFIS is depicted in Fig. 3, in which a circle indicates a fixed node, whereas a square indicates an adaptive node. The ANFIS used in this paper consists of different layers as follows.

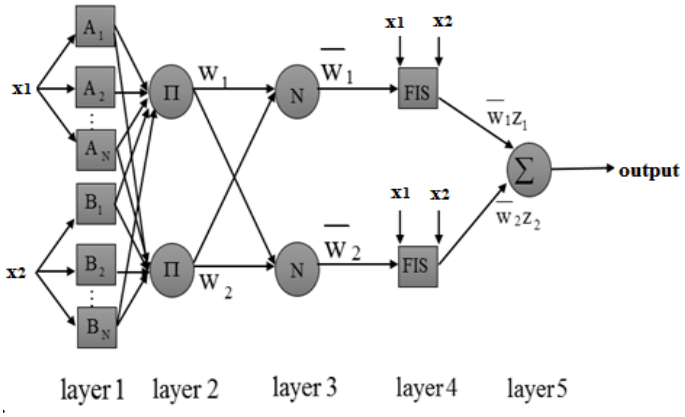

Fig. 3. Schematic of ANFIS modeling approach for nonlinear mapping with two inputs, adapted from [14].

Table 1. Parameters of the arrester in this study.

p(kA)	q	v_{ref}(kA)
1	4	49

Layer 1: In this layer, all inputs are changed into fuzzy inputs. To this end, membership functions of the following form are used.

$$w_i = \mu_{A_i}(x_1)\mu_{B_i}(x_2), i = 1,2 \tag{12}$$

where c_i, σ_i are parameters changing the shape of membership functions and defined in such a way that each membership function has a belongingness value of one at each sampled input and is smoothly decreasing at the neighbor sampled inputs. Variable 'x' is a symbol for each input.

Layer 2. In this layer, the weighting for each rule is computed as below

$$w_i = \mu_{A_i}(x_1)\mu_{B_i}(x_2), i = 1,2 \tag{13}$$

Layer 3. In this layer, all weightings in the previous layer are normalized, that is

$$\overline{w}_i = \frac{w_i}{w_1 + w_2}, i = 1,2 \tag{14}$$

Layer 4. This layer is called TSK fuzzy inference system (FIS). This layer consists of a number of following if-then rules:

$$\text{Rule}: \text{if } x_1 \text{ is } A_i \text{ and } x_2 \text{ is } B_i \text{ then } \text{output} = p_i x_1 + q_i x_2 + k_i \tag{15}$$

where $A_i, i = 1,2,..N$, and $B_i, i = 1,2,..N$ are the membership functions as defined in (1). Also p_i, q_i, k_i are constants determined using least square technique in training process to decrease the predefined error.

Layer 5. In this layer, all weighted outputs of FISs are combined, so that the overvoltage is computed as below

$$\text{Output}(x_1, x_2) = \sum_{i=1}^{2} \overline{w}_i z_i = \sum_{i=1}^{2} \overline{w}_i (p_i x_1 + q_i x_2 + r_i) \tag{16}$$

Further information in this regard can be found in [14

3- SENSITIVITY ANALYSIS

Consider the overhead line in Fig. 1 having length L=1 km, and radius 2.7 cm and terminated to an arrester at right side and matched at left side. There are a number of models for arresters for instance [20, 21]. In this study, without losing generality, it is expressed as a nonlinear resistance [21]. It has been also used in [6, 7].

$$i = p\left(\frac{v}{v_{ref}}\right)^q \tag{17}$$

Where i and v are the arrester voltage and current, respectively; p, q, and v_{ref} are constants. Table 1 tabulates the selected parameters for this arrester the same as [8].

Now, all parameters which may affect the overvoltage are investigated. They are overhead line height (h), resistivity of soil (ρ), length of overhead line (L) and grounding system length (l).

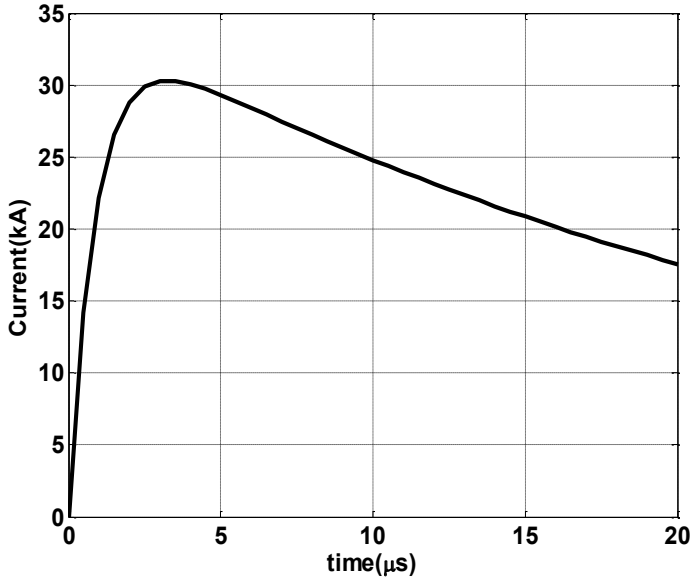

Fig. 4. Typical l waveform for the lightning current in this study and expressed as 2/20μs-30kA [8].

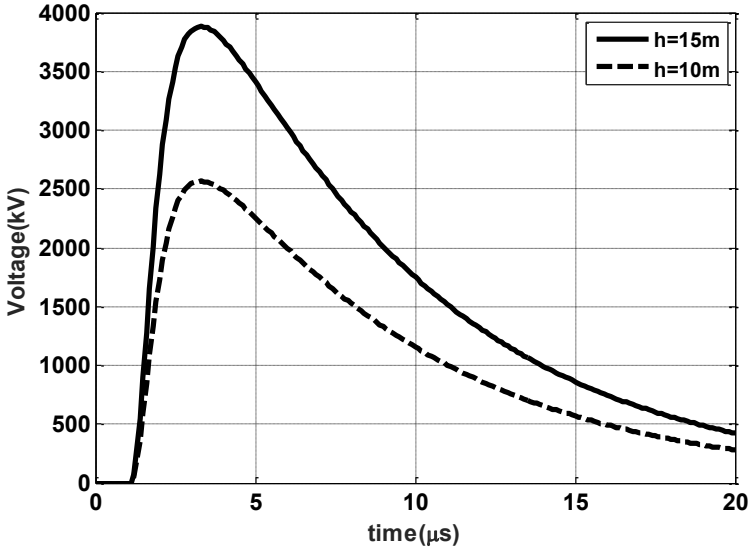

Fig. 5. Variation of transient voltage versus overhead line height (h) under assumption of l=3m, ρ=100 Ωm.

All simulations based on the exact model are carried out by a lightning current with double-exponential waveform, i.e., 2/20μs-30kA as shown in Fig.4. It injects to the middle of the overhead line. Prior to analysis, it is fitted with three sinusoidal waveforms, i.e. k=3, in the time interval of interest.

Figs. 5, 6, and 7 illustrate the variations of the transient voltage versus ρ , h, l. As seen, the three parameters affects the overvoltage so that they can be used as variables. Also, as shown in Fig. 8, the time delay on the transient voltage is created. It is physically due to the EM waves propagation speed. Therefore it is disregarded as an input except for very long length.

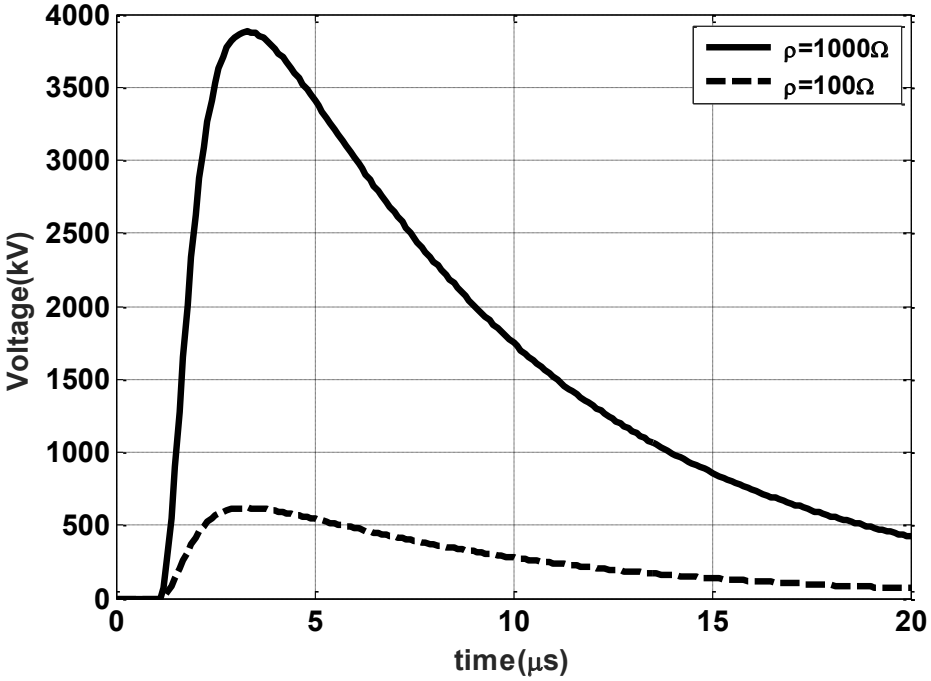

Fig. 6. Variation of transient voltage versus lossy soil resistivity (ρ) under assumption of l=3m, h=10m.

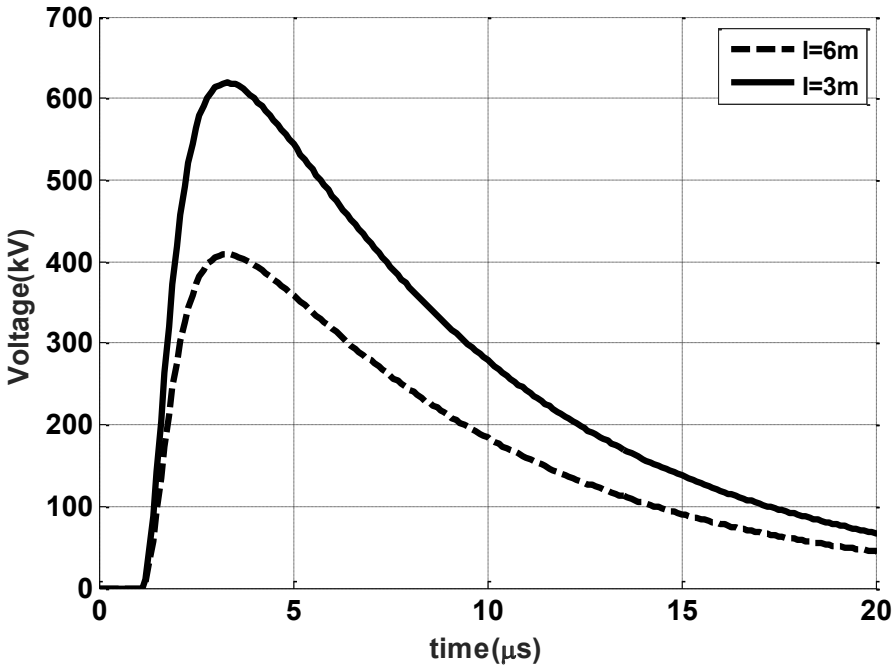

Fig. 7. Variation of transient voltage versus vertical electrode length (l) under assumption of h=10m, ρ=100 Ωm, l=3m.

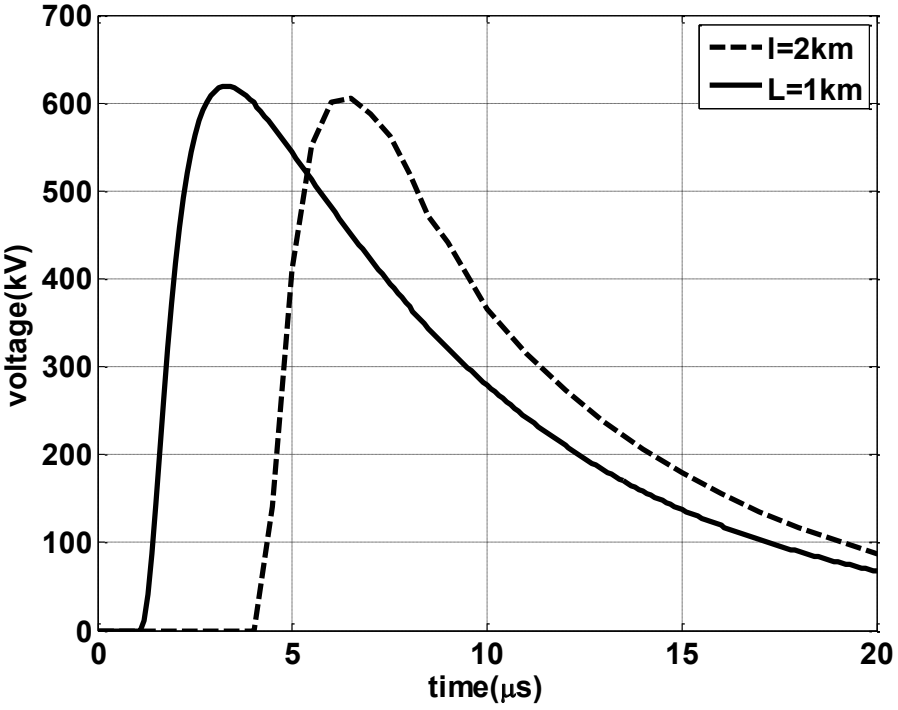

Fig. 8. Variation of transient voltage versus overhead line length (L) under assumption of h=10m, ρ=100 Ωm, l=3m.

4- NUMERICAL RESULTS

According to the above findings, now a closed-form expression for the overvoltage as an output versus the three inputs including h, l, and ρ based on ANFIS technique is extracted. To this end without losing generality, five samples for ρ in the intervals of [100,1000]Ωm, 3 samples for l in the interval of [3,9]m and 9 samples for h in the intervals of [0 ,3]m are first selected. These intervals can be extended. The corresponding outputs are computed based on the exact model [11] and then used in the training process (totally 5×9×3=135 input-output samples are needed). The root mean square error (RMSE) for both grounding systems are shown in Fig. 9. As can be seen, after 10 epochs, the iteration processes for both grounding systems are converged. Accordingly, the adjusted membership functions are extracted and shown in Fig. 10. Now the created ANFIS algorithm can be used for predicting the overvoltage efficiently for arbitrary values of inputs. In prediction phase, assume that the vertical rod is of length $l=3$ m and the grid is an equally-spaced 2×2 square with meshes 5m×5m, while h and ρ are varied.

Figs. 11 and 12 show the ANFIS-based overvoltage respectively when the resistivity is constant and height is variable, and vice versa. In both figures, the simulation results based on the exact model in [11] are also included with the aim of comparison. The comparison shows excellent agreement. Table 1 compares the run times of different models for computing the overvoltage as well. As can be seen, among different models, ANFIS has the lowest run time which is practically of importance.

5- APPLICATION TO COMPLEX SOILS

5- 1- Dispersive Soils

As an application of the proposed model, it can be used in computing overvoltage when the electrical parameters of soil are frequency-dependent (dispersive soil). To this aim, at first, the frequency variations of resistivity and relative dielectric constants of soil are assumed to be computed as below [22]

$$\rho(f)=\rho_0\left(1+\left(1.2.\times10^{-6}\times\rho_0{}^{0.73}\right)\left(f-100\right)^{0.65}\right)^{-1} \tag{18}$$

$$\varepsilon_r(f)=\begin{cases}192.2 & f\le 10\text{kHz}\\ 1.3+7.6.10^3.f^{-0.4} & f\ge 10\text{kHz}\end{cases} \tag{19}$$

In (18) and (19), ρ_0 and f are respectively low-frequency resistivity of soil in Ωm and frequency in Hz.

With reference to [15], the inclusion of soil dispersion can be approximately considered at the equivalent frequency $f_{eq}=1/4T_f$ where T_f is the rise time of the lightning current waveform. For the lightning current as shown in Fig. 10, it is 31.25 KHz which leads to the equivalent resistivity and relative dielectric constant respectively $\rho_{eq}=400\Omega$m and $\varepsilon_{req}=127$. Now substituting ρ_{eq} instead of ρ, the overvoltage can be easily computed in dispersive soils. Figs.

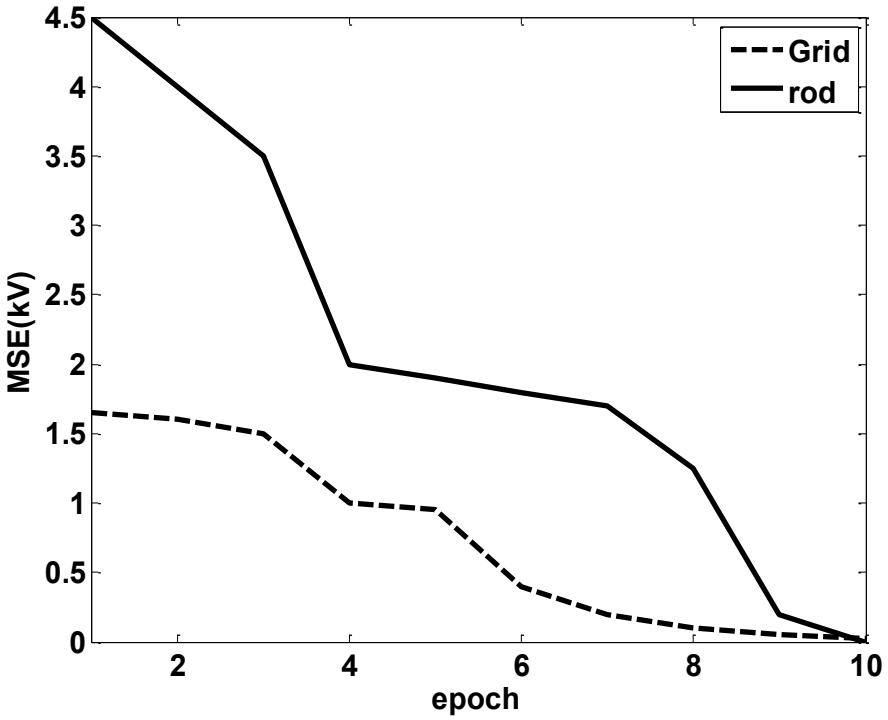

Fig. 9. Mean square errors (MSE) versus epoch in the training process for the rod and grid networks.

13 and 14 show the overvoltage across the arrester based on the ANFIS model and the ones in [23] versus the height and low-frequency resistivity. As can be seen in Fig. 13, good agreement between the ANFIS and [23] is achieved, whereas in Fig. 15, when the height is increased the results of the ANFIS and [23] are diverged since in [23] the Norton's circuit parameters are computed based on BLT equations which are restricted to condition kh<<1.

Evidently, such violation will be more increased for fast-front currents since this condition is no longer satisfied.

5- 2- Two-Layer Soils

As another application of the closed-form expression achieved for the overvoltage, it can be used in horizontally two-layered soil. To this end, the equivalent resistivity concept [16] as expressed in (20) can be used.

$$\rho_{eq}=\rho_1\left[\frac{(\sqrt{\rho_2}+\sqrt{\rho_1})+(\sqrt{\rho_2}-\sqrt{\rho_1})e^{-2d\sqrt{\pi f\mu_0/\rho_1}}}{(\sqrt{\rho_1}+\sqrt{\rho_2})-(\sqrt{\rho_2}-\sqrt{\rho_1})e^{-2d\sqrt{\pi f\mu_0/\rho_1}}}\right]^2 \tag{20}$$

In (18), ρ_1 and ρ_2 are respectively resistivity of the upper and lower layers. Also, d is denoted for upper layer thickness. The frequency f in (20) is equal to 124 kHz for the first stroke current and 516 kHz for the subsequent stroke current [24]. As stated in [16], this approximation leads to good agreement, except that the difference of the resistivity values of the two layers is increased and the upper layer thickness is decreased. The error will be more pronounced for subsequent stroke current (see Table I and Fig. 4 in [16]).

Integration of this approximation with the time-consuming finite difference time domain method (FDTD) has been used for transient analysis of the overhead lines over two-layer soils in the absence of arresters successfully [25].

To investigate the validity of the proposed model in two-layer soils, it is assumed that the resistivity values of the upper and lower layers are $\rho_1=1000\Omega m$ and $\rho_2=100\Omega m$ respectively. Fig. 15 shows the ANFIS-based overvoltage across the arrester versus the upper layer thickness. In addition, the overvoltage in single-layer soils are included. As can be seen, except for the low-valued thickness, good agreement between the ANFIS model and [26] is achieved.

5- 3- Dispersive and Two-Layer Soils

Finally, the efficient expression can be used in soils where dispersion and non-homogeneity simultaneously occur. To this aim, low-frequency equivalent resistivity, i.e. ρ_{0eq}, instead of ρ_0 in (20) is replaced

$$\rho_{0eq}=\rho_{01}\left[\frac{(\sqrt{\rho_{02}}+\sqrt{\rho_{01}})+(\sqrt{\rho_{02}}-\sqrt{\rho_{01}})e^{-2d\sqrt{\pi f\mu_0/\rho_{01}}}}{(\sqrt{\rho_{01}}+\sqrt{\rho_{02}})-(\sqrt{\rho_{02}}-\sqrt{\rho_{01}})e^{-2d\sqrt{\pi f\mu_0/\rho_{01}}}}\right]^2 \tag{21}$$

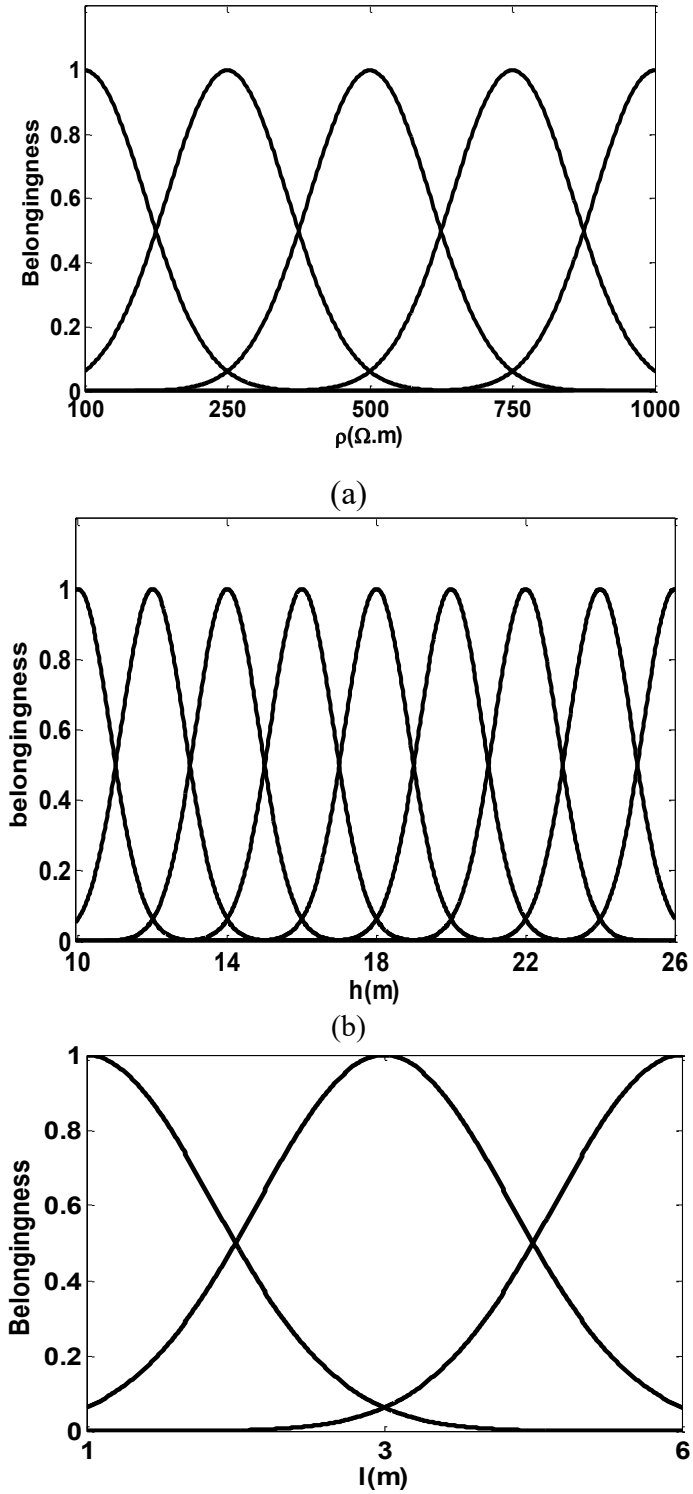

Fig. 10. Adjusted membership functions versus the three input variables, (a): , (b): h, and (c): l.

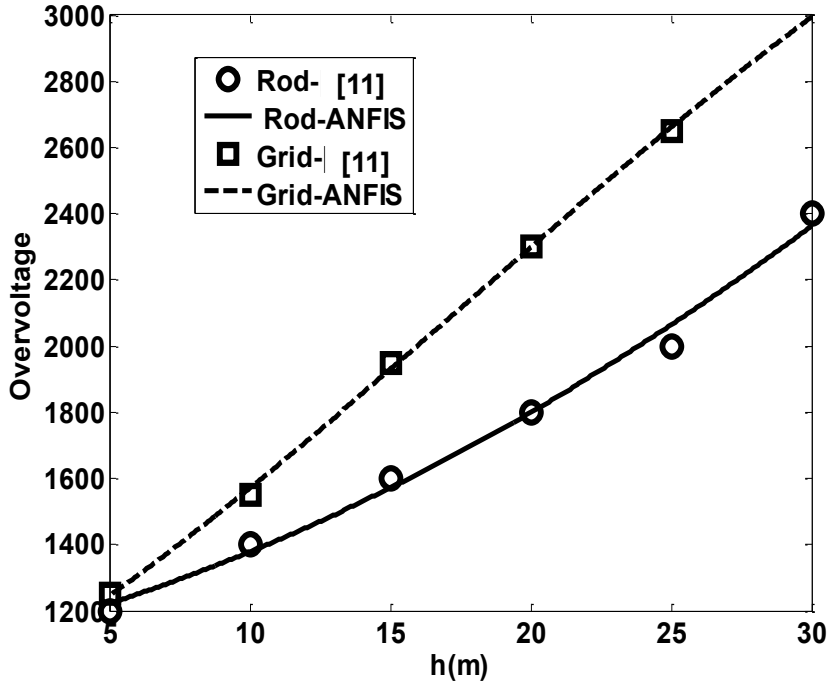

Fig. 11. Comparison of predicted overvoltages (kV) based on the ANFIS and [11] with $\rho = 500\Omega m$.

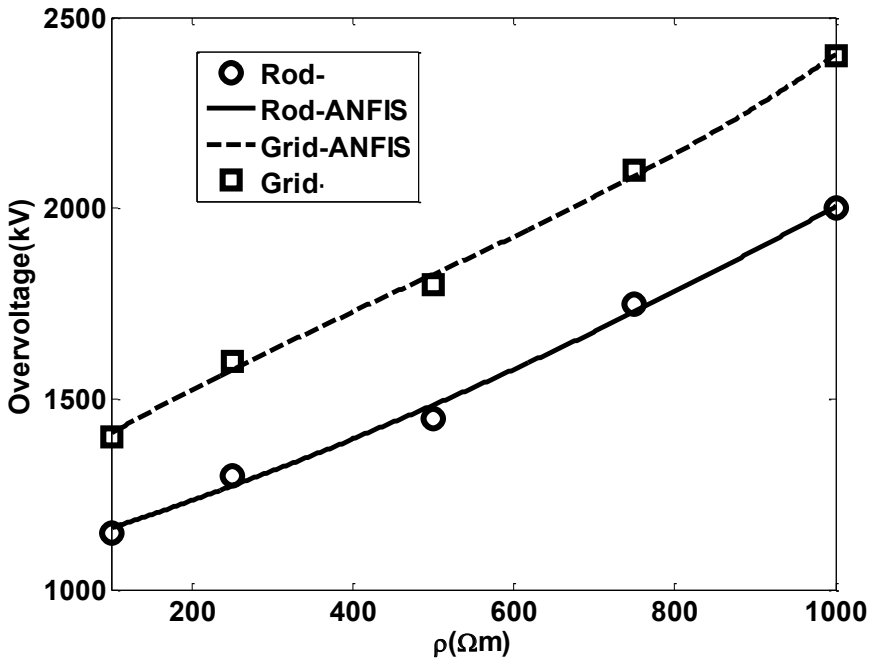

Fig. 12. Comparison of predicted overvoltages based on the ANFIS and [11] with h=10m.

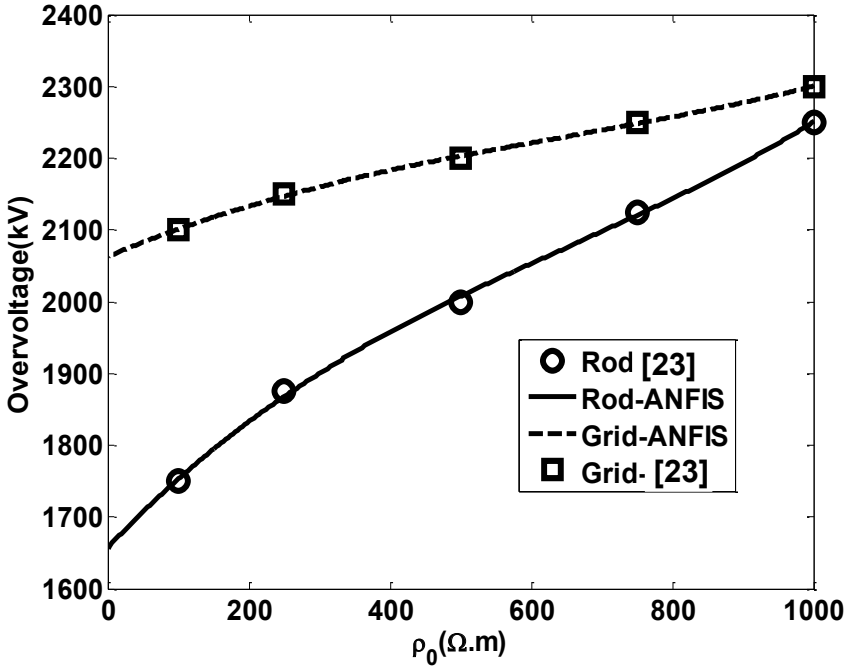

Fig. 13. Predicted overvoltages based on the ANFIS model and [23] in dispersive soils versus the low-frequency resistivity (ρ_0) under assumption of h=0 .

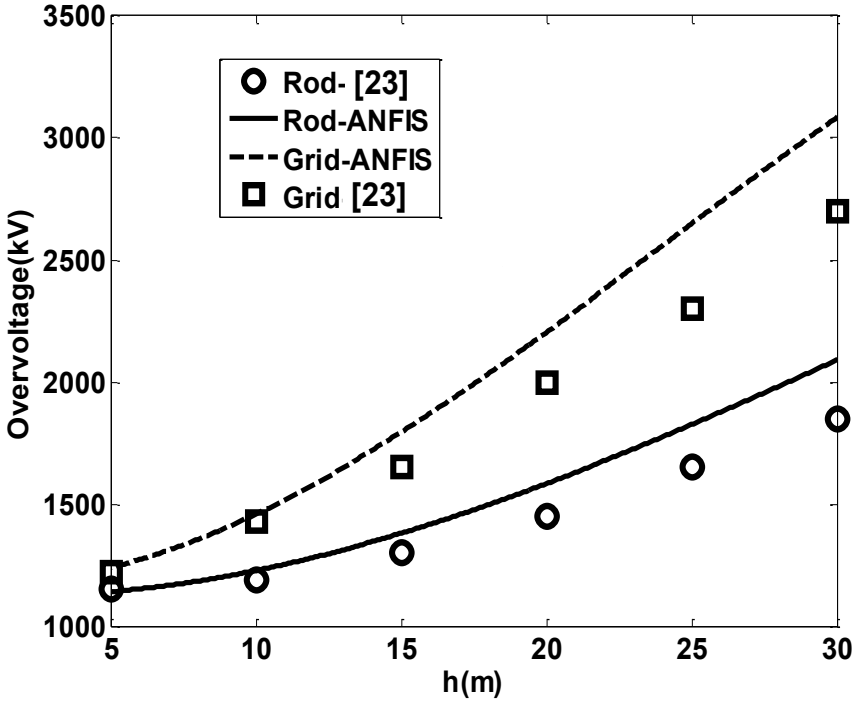

Fig. 14. Predicted overvoltages based on the ANFIS model and [23] in dispersive soils versus the height of the transmission line (h) under the assumption of $\rho_0 = 500\Omega$.

Table 2. Comparison of run times (sec) of the different methods for computing the overvoltage.

Method		[11]	BLT-AOM [7]	This paper
Ground	Rod	9	19	0.45
	Grid	11	21	0.45

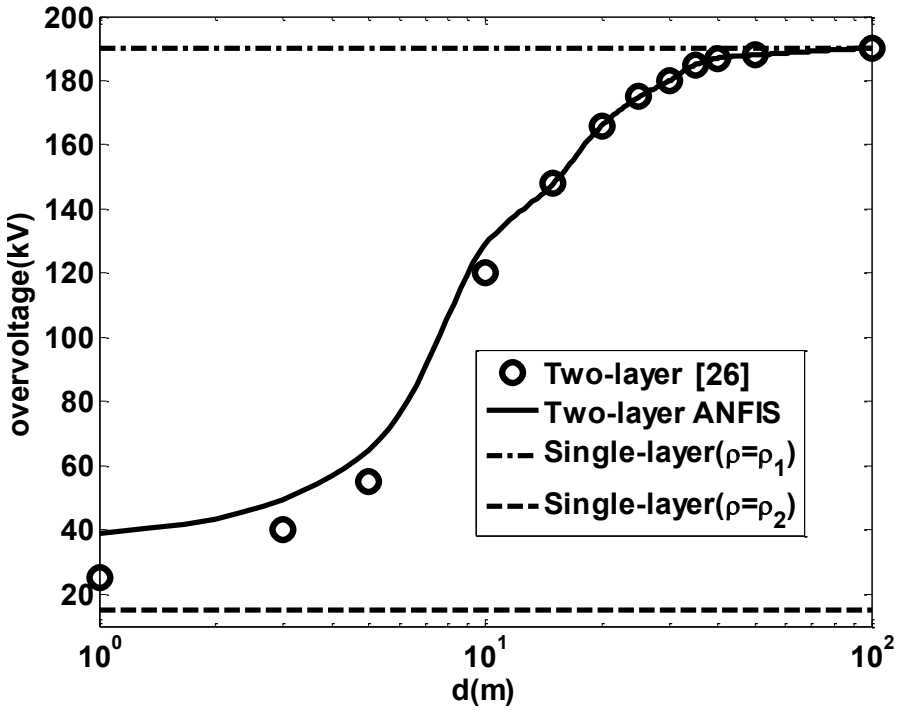

Fig. 15. ANFIS-based overvoltages versus the upper layer thickness in two-layer soils and comparison with [26] as well as single-layer ones.

To illustrate this situation of soil, it is assumed that the low-frequency resistivity values of upper and lower layers are respectively 1000Ωm and 100Ωm. the upper layer thickness is assumed to be 10m. Fig. 16 shows the overvoltage for such soil. With the aim of comparison, the single-affected soils including dispersive single-layer soils with low-frequency resistivity equal to the low-frequency resistivity of the upper and lower layers (ρ_0=1000, 100Ωm) and non-dispersive two-layer soil (ρ_1=1000, ρ_2=100Ωm) are included in this figure as well. From this figure, two notes are inferred. The first is that the overvoltage in dispersive and two-layer soil is a middle value between the individual ones in dispersive and single-layer soils having the low-frequency resistivity of upper and lower layers. The second is that the overvoltage in dispersive and two-layer soil is greater than that of non-dispersive and two-layer soil. The mentioned findings play an important role in selecting lightning arresters which should be considered by power engineers.

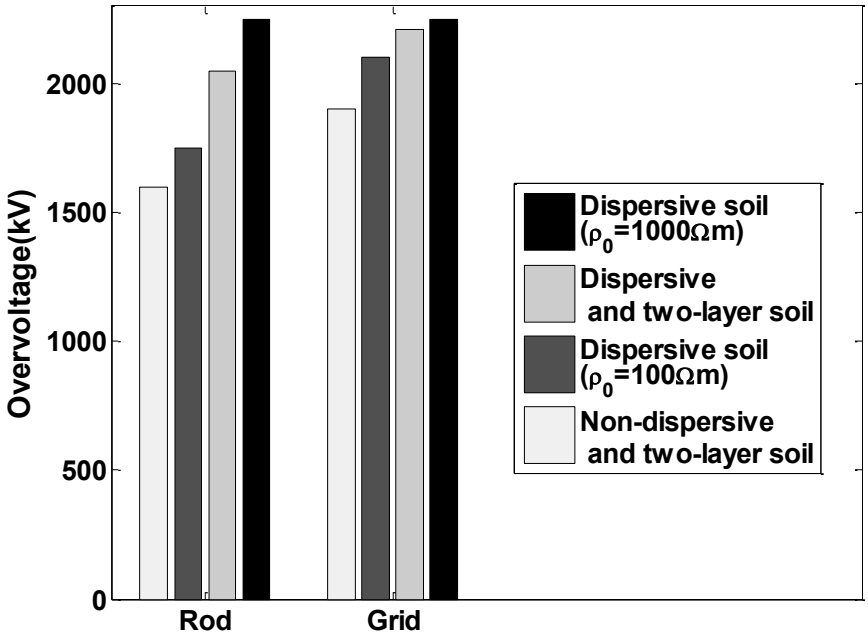

Fig. 16. ANFIS-based overvoltages in dispersive and two-layer soils and comparison single-affected soils.

6- conclusion

In this paper, the application of the ANFIS algorithm was proposed for comprehensive and broad-band prediction of overvoltage of single-phase overhead lines terminated with arresters. The electrical parameters of the lossy soil can be constant, frequency-dependent, and in-homogenous. Due to its efficiency, it plays an important role when the weather conditions are changed since repetitive and time-consuming computations are removed.

Extending the proposed model to single and three-phase overhead lines considering the nonlinear phenomenon of ionization and front time is in progress. In such cases, ANFIS technique may be violated results since the number of inputs increased. To remove this drawback, spatial membership functions [27, 28] can be used.

References

[1] IEEE Guide for the Application of Insulation Coordination, IEEE Standard 1313.2, 1999.

[2] M. Akbari, and K. Sheshyekani, "The Effect of an Ocean-Land Mixed Propagation Path on the Lightning Electromagnetic Fields and Their Induced Voltages on Overhead Lines", IEEE Transactions on Electromagnetic. Compatibility, vol. 55, no. 6, pp. 1-8, 2014.

[3] M. Akbari, and K. Sheshyekani, "Evaluation of Lightning Electromagnetic Fields and Their Induced Voltages on Overhead Lines Considering the Frequency Dependence of Soil Electrical Parameters", IEEE Transactions on Electromagnetic. Compatibility, vol. 55, no. 6, pp. 1210-1219, 2013.

[4] Fernando H. Silveira, Silverio Visacro, Rafael Alipio, and Alberto De Conti, "Lightning-Induced Voltages Over Lossy Ground: The Effect of Frequency Dependence of Electrical Parameters of Soil", vol. 56, no. 5, pp. 1129-1136, 2014.

[5] S. R. Ostadzadeh, and S. Mehrabi, "Impact of Ocean-Land Mixed Propagation Path on Equivalent Circuit of Grounding Rods", Journal of Communication Engineering, vol. 8, no. 2, pp. 1-11, 2019.

[6] H. Janani, R. Moini, and S. H. H. Sadeghi, "Evaluation of Lightning-Induced Voltage on Overhead Lines with Nonlinear Loads using the Scattering Theory", IEEE Transactions on Power Delivery, vol. 21, no. 1, pp. 31-324, 2012.

[7] M. Namdari, M. Khosravi-Farsani, R. Moini, and S. H. H. Sadeghi, "An Efficient Parallel 3-D Method for Calculating Lightning-Induced Disturbances on Overhead Lines in the Presence of Surge Arresters", IEEE Transactions on Electromagnetic Compatibility, vol. 5, no. 10, pp. 259-267, 2016.

[8] K. Sheshyekani, S. H. H. Sadeghi, R. Moini, F. Rachidi, M. Paolone," Analysis of transmission lines with arrester termination, considering the frequency-dependence of grounding systems" IEEE Transactions on Electromagnetic. Compatibility, vol. 51, no. 4, pp. 986-994, 2009.

[9] F. Rachidi "A Review of Field-to-transmission line coupling models with special emphasis to lightning-induced voltages on overhead lines" IEEE Trans. on Electromagn. Compat, vol. 54, no. 4, pp. 898–911, August 2012.

[10] F. P. Hart, D. G. Stephenson, C. R. Chang, K. Gharaibeh, R. G. Johnson, and M. B. Steer, "Mathematical foundations of frequency-domain modeling of nonlinear circuits and systems using the arithmetic operator method," Int. J. RF Microw. Comput.-Aided Eng., vol. 13, no. 6, pp. 473–495, Nov. 2003.

[11] S. M. Taghavi, S. R. Ostadzadeh, and S. H. H. Sadeghi, "An Efficient Spectral Balance Method for Transient Analysis of Single Phase Overhead Lines in the Presence of Surge Arresters", Inter J. Numer Model, Electronic Networks, Devices, vol. 34, no. 1, pp. 1-15, 2021.

[12] J. Osvaldo S. Paulino et al, "The Peak Value of Lightning-Induced Voltages in Overhead Lines Considering the Ground Resistivity and Typical Return Stroke Parameters", IEEE Transactions on Power Delivery, vol. 26, no. 2, pp. 920-927, 2010.

[13] Jun Guo, Yan-zhao Xie, and Ai-ci Qiu, "Calculation of Lightning Induced Voltages on Overhead Lines Using an Analytical Fitting Representation of Electric Fields", IEEE Transaction on Electromagnetic Compatibility, vol. 27, no. 2, pp. 927-935, 2017.

[14] V. Aghajani1, and S. S. Sajjadi, Saeed Reza Ostadzadeh, "Design of Grounding Vertical Rods Buried in Complex Soils Based on Adaptive Network-Based Fuzzy Inference Systems", Journal of Communication Engineering, Vol. 7, No. 2, July-December 2018.

[15] Mehrdad Mokhtari, Zulkurnain Abdul-Malek, and Chin Leong Wooi, "Integration of Frequency Dependent Soil Electrical Properties in Grounding Electrode Circuit Model", International Journal of Electrical and Computer Engineering (IJECE), vol. 6, no. 2, pp. 792~799, April 2016.

[16] D. A. Tsiamitros, G. K. Papagiannis, and P. S. Dokopoulos, "Homogenous Earth Approximation of Two-Layer Earth Structures: An Equivalent Resistivity Approach," IEEE Trans. on Power Delivery, vol. 22, no. 1, pp. 658-666, 2007.

[17] Bahrami A, Ostadzadeh S.R. "Back scattering from single, finite, and infinite array of nonlinear antennas based on intelligent water drops", Int. J Comput Math Electr Electron Eng. vol. 38, pp. 2040-2056, 2019.

[18] Samiian H, Ostadzadeh S.R, Mirzaie A. Application of intelligent water drops in transient analysis of single conductor overhead lines terminated to grid-grounded arrester under direct lightning strikes. J Commun Eng., vol. 5, no. 1, pp.50-59, 2016.

[19] Bahrami A, Ostadzadeh S.R, "Comprehensively efficient analysis of nonlinear wire scatterers considering lossy ground and multi-tone excitations", The Applied Computational Electromagnetics Society Journal (ACES), vol. 35, no. 8, pp. 878-886, 2020.

[20] J. A. Martinez and D.W. Durbak, "Parameter determination for modeling systems transients-Part V: Surge arresters," IEEE Trans. Power Del., vol. 20, no. 3, pp. 2073–2078, Jul. 2005.

[21] IEEE Fast Front Transients Task Force, "Modeling guidelines for fast front transients," IEEE Trans. Power Del., vol. 11, no. 1, pp. 493–506, Jan. 1996.

[22] S. Visacro and Rafael Alipio, "Frequency dependence of soil parameters: Experimental results, predicting formula and influence on the lightning response of grounding electrodes", IEEE Transaction on Electromagnetic Compatibility, vol. 27, no. 2, pp. 927-935, 2012.

[23] H. Yazdi, S. R. Ostadzadeh, and F. Taheri Astaneh, "Transient Analysis of Single-Conductor Overhead Lines Terminated to Grounded Arrester Considering Frequency Dependence of Electrical Parameters of Soil using Genetic Algorithm," Journal of Applied Electromagnetics, vol. 3, no. 2, pp. 35-42, 2015. (In Persian).

[24] IEEE Guide for Improving the Lightning Performance of Electric Power Overhead Distribution lines. Approved 28 January 2011, IEEE Standards Board. IEEE Std 1410TM- 2010.

[25] José Osvaldo S. Paulino, Wallace C. Boaventura, Celio Fonseca Barbosa, "An Approximate Expression for the Equivalent Resistivity of a Two-Layer Soil", 2013 International Symposium on Lightning Protection (XII SIPDA), Belo Horizonte, Brazil, pp. 7-11, 2013.

[26] S. Mehrabi, and S. R. Ostadzadeh, "Validity of RLC Equivalent Circuit of Grounding Electrodes in Combination with Equivalent Resistivity in Two-layer Soils and Its Application in Transient Analysis of Arrester-Connected Overhead Lines under Lightning Strike", Journal of Applied Electromagnetics, vol. 9, no. 1, pp. 35-42, 2021. (In Persian)

[27] S. R. Ostadzadeh, "Qualitative model of the input impedance of rectangular microstrip antenna", J Fuzzy Set Valued Anal. , vol. 2, pp. 154-165, 2015.

[28] S. R. Ostadzadeh, "Nonlinear analysis of nonlinearly loaded dipole antenna in the frequency domain using fuzzy inference", J Commun. Eng. vol. 6, no. 1, pp. 26-28, 2017.

HOW TO CITE THIS ARTICLE

S. R. Ostadzadeh, Application of ANFIS Technique for Wide-Band Modeling of Overvoltage of Single-Conductor Overhead Lines with Arrester above Dispersive and Two-Layer Soils, AUT J Electr Eng, 55(2) (2023) 241-254.

DOI: 10.22060/eej.2023.22360.5536